

Synthesis and Characterization of 2,9-Bis(perfluorobutyl)pentacene as an n-Type Organic Field-Effect Transistor

Kazuo Okamoto,[1] Kenji Ogino,*[1] Mitsuaki Ikari,[2] and Yoshihito Kunugi[2]

[1]Graduate School of Bio-Applications and Systems Engineering, Tokyo University of Agriculture and Technology, Koganei, Tokyo 184-8588

[2]Department of Applied Chemistry, Faculty of Engineering, Tokai University, 1117 Kitakaname, Hiratsuka 259-1292

Received November 7, 2007; E-mail: kogino@cc.tuat.ac.jp

A novel organic semiconductor, 2,9-bis(perfluorobutyl)pentacene, was synthesized in seven steps, and was characterized by NMR, IR, and UV spectroscopy. From differential scanning calorimetry analyses, no liquid crystalline phase was observed, unlike 2,9-dibutylpentacene. The morphology of thin films formed at different substrate temperatures was investigated by atomic force microscopy (AFM) and X-ray diffraction analysis. Organic field-effect transistors (OFETs) fabricated with this compound showed electron mobility of $1.7 \times 10^{-3}\,cm^2\,V^{-1}\,s^{-1}$ using Ag source–drain electrodes.

Organic field-effect transistors (OFETs) are of great interest because of their potential applications including low-cost, large-area, and flexible electronic devices, such as pliable electronic papers, RFID tags, and flexible OLEDs.[1–3] OFETs based on linear acenes,[4–7] oligothiophenes,[8] and regioregular poly(3-hexylthiophene)[9] have been extensively studied. Various devices showing high-performance exceeding that of amorphous silicon based devices, have been developed. Most of the above-mentioned materials are p-type organic semiconductors, in which holes are the predominant carriers. Development of high-performance OFETs based on n-type organic materials is also very important because the combination of p- and n-type materials enables the fabrication of complementary logic circuits[10] and ambipolar transistors.[11]

As n-type materials, C_{60} derivatives,[12] fluorinated copper phthalocyanine (F16CuPc),[13] terthiophene-based quinodimethane,[14] naphthalenetetracarboxamide derivatives,[15] perylene tetracarboxamide,[16] thiazole oligomers,[17] and perfluoropentacene[18] have been reported. It is well known that perfluorination of p-type materials is an effective way to produce n-type materials. This is because enhancement of electron injection is assured by the introduction of highly electronegative fluorine atoms. Alternatively it has also been reported that substitution of p-type oligothiophene cores with perfluoroalkyl groups[19] or perfluorobenzoyl[20] groups affords effective n-type materials.

We have previously reported that liquid crystallinity appeared over a relatively wide temperature range by the introduction of alkyl groups at the 2 and 9 positions of pentacene.[21] For example, 2,9-dibutylpentacene shows crystal–liquid crystal phase transition at 115 °C, and is converted to isotropic phase at 194 °C. In this paper, we report the synthesis and characterization of 2,9-bis(perfluorobutyl)pentacene as an n-type analogue of 2,9-dialkylpentacenes. For the synthesis of unsubstituted or symmetrically tetra-substituted pentacene, a conventional synthetic scheme has been utilized, where pentacenequinone derivatives are prepared by the condensation of 1,4-cyclohexanedione and phthalaldehyde derivatives, and subsequent reduction gives pentacene derivatives.[22] This is a high yielding reaction and the starting materials are readily available, but it is not applicable to the synthesis of 2,9-disubstituted pentacenes with high purity because of formation of two isomers. Therefore, a synthetic route starting from pyromellic anhydride and consisting of seven steps is proposed for a highly pure product with no isomer contamination. It is crucial that no isomers are produced in the synthesis of organic transistor materials, because the existence of a trace of isomers disturbs the regular packing of the crystal.[23] The introduction of perfluoroalkyl groups transforms the originally p-type pentacene derivative to the desired n-type compound. The thermal properties of the synthesized compound are described in comparison with the alkyl analogue. The crystallinity and morphology of thin films deposited at different substrate temperatures are also discussed. n-Type OFETs based on 2,9-bis(perfluorobutyl)pentacene with different source and drain electrodes were fabricated and characterized.

Experimental

General. All reagents were purchased from Wako Pure Chemical Industries, Ltd. and were used without further purification. Column chromatography was performed on silica gel 60N (spherical, neutral, 63–210 μm) purchased from KANTO Chemical Co., Inc. All compounds were characterized by a combination of MS spectroscopy (Shimadzu, GCMS-QP2010), ^1H, ^{13}C, and ^{19}F NMR, spectroscopy (Varian Mercury Plus 400 MHz), and IR spectroscopy (Shimadzu, FTIR-8300). Chemical shifts are reported as δ values (ppm) relative to internal tetramethylsilane (^1H and ^{13}C NMR,) or hexafluorobenzene (^{19}F NMR). UV–vis spectra were recorded on a Shimadzu, UV-3101PC for solution and thin film. Thermal properties were investigated by differential scanning calorimetry (DSC, TA Instruments Q10) under nitrogen flow, and thermogravimetric analysis (TGA, ULVAC-RIKO, Inc. VAP-9000). The thin films of 2,9-bis(perfluorobutyl)pentacene were characterized by X-ray diffraction (XRD) analysis using a Philips PW1830 X-ray diffractometer. XRD patterns were obtained using

Published on the web April 10, 2008; doi:10.1246/bcsj.81.530

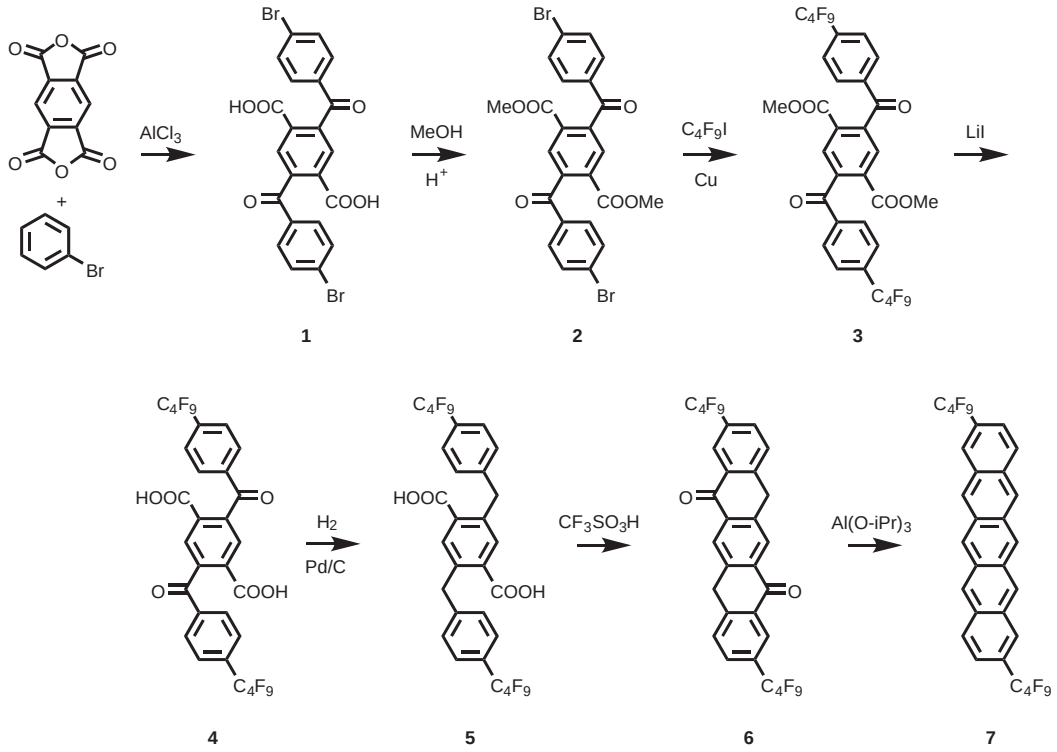

Figure 1. Synthesis of 2,9-bis(perfluorobutyl)pentacene.

Bragg–Brenano geometry (θ–2θ) with Cu Kα radiation as an X-ray source with an acceleration voltage of 40 kV and a beam current of 30 mA. The film morphology was observed by atomic force microscopy (AFM), using a Digital Instruments NanoScope IIIa in the tapping mode.

Synthesis. Figure 1 shows the synthetic route of 2,9-bis(perfluorobutyl)pentacene used in this study.

Synthesis of 2,5-Bis(4-bromobenzoyl)terephthalic Acid (1): A mixture of 24.0 g (110 mmol) of pyromellic anhydride and 150 mL of bromobenzene was heated at 45 °C under a nitrogen atmosphere. To the mixture was added 40.0 g (300 mmol) of aluminum chloride in small portions. After stirring for 6 h at 45 °C, the reaction mixture was poured into a mixture of 400 g of ice and 180 mL of concentrated hydrochloric acid and was stirred 1 h at room temperature. The organic layer was extracted with 400 mL of ethyl acetate and 400 mL of tetrahydrofuran (THF). The extract was washed by three 400 mL portions of water and was dried over anhydrous magnesium sulfate. After evaporation of solvents, the light yellow crude product was washed with 150 mL of ethyl acetate, and dried to give 12.5 g of white powder. This was recrystallized from methanol to afford 2,5-bis(4-bromobenzoyl)terephthalic acid as white powder (3.0 g, 5%). ^{1}H NMR (400 MHz, DMSO, δ): 7.67 (4H, d, $J = 8.5$ Hz), 7.74 (4H, d, $J = 8.5$ Hz), 7.95 (2H, s). ^{13}C NMR (100 MHz, $CDCl_3$, δ): 194.2, 165.6, 141.8, 135.4, 133.4, 131.9, 131.0, 128.9, 127.7. FT-IR (KBr): 3423, 3059, 2654, 2588, 2542, 1697, 1585, 1499, 1398, 1364, 1298, 1252, 1178, 1121, 1070, 1011, 945, 914, 841, 795, 563 cm^{-1}.

Synthesis of Dimethyl 2,5-Bis(4-bromobenzoyl)terephthalate (2): A mixture of 34.0 g (64 mmol) of compound **1**, 200 g of methanol, 850 mL of toluene, and 8.5 mL of sulfuric acid was refluxed overnight. The reaction mixture was cooled to room temperature, and 1000 mL of methanol was added. Precipitate was collected and washed with 300 mL of cold methanol, and was dried to give 22.4 g of white powder (63%). ^{1}H NMR (400 MHz, $CDCl_3$, δ): 3.70 (6H, s), 7.64 (8H, s), 8.05 (2H, s). ^{13}C NMR (100 MHz, $CDCl_3$, δ): 52.9, 129.1, 129.5, 130.8, 132.2, 132.5, 135.2, 142.5, 164.6, 194.2. FT-IR (KBr): 3090, 3059, 3024, 3003, 2949, 2845, 1720, 1682, 1585, 1481, 1437, 1398, 1381, 1308, 1271, 1177, 1113, 1067, 1007, 974, 945, 914, 845, 820, 793, 741, 685, 573 cm^{-1}.

Synthesis of Dimethyl 2,5-Bis(4-perfluorobutylbenzoyl)terephthalate (3): A mixture of 2.0 g (3.5 mmol) of compound **2**, and 2.0 g of copper powder in 50 mL of dimethyl sulfoxide (DMSO) was heated at 120 °C under nitrogen atomosphere. A solution of 27.5 mL (10 mmol) of perfluorobutyl iodide in 70 mL of DMSO was added over 2.5 h. The reaction mixture was stirred for 2 h at 120 °C. The mixture was cooled to 60 °C, and was poured into 300 mL of chloroform. Precipitate was purified by column chromatography (silica gel, dichloromethane), and dried to give 2.5 g of white powder (85%). ^{1}H NMR (400 MHz, $CDCl_3$, δ): 3.70 (6H, s), 7.73 (4H, d, $J = 8.5$ Hz), 7.92 (4H, d, $J = 8.5$ Hz), 8.11 (2H, s). ^{19}F NMR (376 MHz, $CDCl_3$, δ): 36.3 (4F, m), 39.3 (2F, q), 50.4 (4F, t, $J = 12$ Hz), 80.8 (6F, m). FT-IR (KBr): 3050, 2905, 1720, 1684, 1441, 1412, 1354, 1310, 1267, 1246, 1226, 1204, 1192, 1170, 1136, 1113, 947, 868, 824, 795, 750, 710, 687 cm^{-1}.

Synthesis of 2,5-Bis(4-perfluorobutylbenzoyl)terephthalic Acid (4): A mixture of 5.0 g (5.96 mmol) of compound **3** and 10 g (74.7 mmol) of lithium iodide in 250 mL of dimethyl formamide (DMF) was heated at 150 °C for 12 h under nitrogen atmosphere. After cooling to room temperature, the reaction mixture was poured into 300 mL of 2 M hydrochloric acid. Precipitate was washed twice with 300 mL of water, and dried to give 4.4 g (5.43 mmol) of white powder (91%). ^{1}H NMR (400 MHz, DMSO, δ): 7.86 (2H, d, $J = 8.4$ Hz), 7.97 (2H, d, $J = 8.3$ Hz), 8.07 (1H, s). ^{19}F NMR (376 MHz, DMSO, δ): 37.4 (4F, t, $J = 13.3$ Hz), 40.3 (4F, q, $J = 8.7$ Hz), 52.3 (4F, t, $J = 11.9$ Hz), 82.0 (6F, t, $J = 9.2$ Hz). FT-IR (KBr): 3418, 3053, 2860, 2671, 2559, 1697, 1493, 1412, 1354, 1306, 1240, 1136, 1111, 1090,

1022, 1005, 987, 953, 914, 887, 868, 843, 824, 800, 787, 748, 717, 584 cm^{-1}.

Synthesis of 2,5-Bis(4-perfluorobutylbenzyl)terephthalic Acid (5): A mixture of 5.39 g (6.6 mmol) of compound **4** and 8.35 g of 5% palladium on carbon (NX-Type: bought from N.E. Chemcat Corporation) in 540 mL of THF was heated at 60 °C for 24 h under an atmosphere of hydrogen at 0.4 MPa. After the reaction, the mixture was filtered through Celite® to remove the catalyst. The filtrate was concentrated in vacuo. The crude product was purified by washing with 100 mL of hexane, and was dried to give 4.78 g of white powder (93%). ^{1}H NMR (400 MHz, DMSO, δ): 4.44 (4H, s), 7.37 (4H, d, $J = 8.0$ Hz), 7.55 (4H, d, $J = 8.0$ Hz), 7.77 (2H, s). ^{19}F NMR (376 MHz, DMSO, δ): 37.4 (4F, m), 40.3 (4F, t, $J = 8.6$ Hz), 53.1 (4F, d, $J = 13.2$ Hz), 82.1 (6F, m). FT-IR (KBr): 3422, 3017, 2905, 2652, 2540, 2365, 1697, 1616, 1556, 1516, 1499, 1418, 1354, 1271, 1236, 1204, 1132, 1092, 1030, 1005, 987, 920, 872, 851, 797, 743, 689, 590, 532 cm^{-1}.

Synthesis of 3,10-Bis(perfluorobutyl)pentacene-5(14*H*),-12(7*H*)-dione (6): A mixture of 9.1 g (11.6 mmol) of compound **5** and 45 mL of trifluoromethanesulfonic acid was stirred under nitrogen atmosphere overnight at room temperature. The mixture was poured into 350 g of ice and 350 g of water. The precipitate was collected by filtration and washed with 350 mL of 5% aqueous sodium carbonate and then twice with 750 mL of water. The precipitate was dried to give 7.4 g (9.91 mmol) of dark brown powder (86%). Due to the insolubility in appropriate organic solvents, no NMR data were obtained. FT-IR (KBr): 3050, 2905, 1751, 1655, 1616, 1448, 1394, 1354, 1344, 1246, 1205, 1228, 1088, 976, 951, 868, 881, 808, 756, 741, 692, 671, 608, 582 cm^{-1}. MS (EI, 70 eV): m/z (%) = 746 (M^+, 100), 744 (26), 577 ($M^+ - C_3F_7$, 53), 575 (28), 527 ($M^+ - C_4F_9$, 50), 408 ($M^+ - C_6F_{14}$, 6), 406 (26), 358 ($M^+ - C_8F_{18}$, 28), 204 (53), 179 (24).

Synthesis of 2,9-Bis(perfluorobutyl)pentacene (FBP) (7): A mixture of 1.0 g (1.34 mmol) of compound **6** and 20 g (0.99 mol) of aluminum isopropoxide in 200 mL of cyclohexanol was heated to 160 °C with distilling out isopropanol, and then was refluxed for 24 h under argon atmosphere. After cooling to room temperature, the resulting precipitate was collected by centrifugal separation. The precipitate was successively washed with 150 mL of acetic acid, 150 mL of concentrated hydrochloric acid, 150 mL of water, 150 mL of acetone, 150 mL of THF, and 150 mL of methanol, then was dried to give 0.25 g (26.1%) of dark blue powder. ^{1}H NMR (400 MHz, $C_2D_2Cl_2$, 100 °C, δ): 7.40 (2H, d, $J = 9.5$ Hz), 8.02 (2H, d, $J = 9.5$ Hz), 8.24 (2H, s), 8.73 (2H, s), 8.81 (2H, s), 9.03 (2H, s). ^{19}F NMR (376 MHz, $C_2D_2Cl_2$, 100 °C, δ): 37.1 (4F, m), 40.1 (4F, m), 51.5 (4F, m), 81.1 (6F, m). FT-IR (KBr): 3050, 1356, 1261, 1231, 1219, 1200, 1086, 1022, 916, 899, 835, 822, 791, 739, 714, 696, 608, 581, 534, 465 cm^{-1}. MS (EI, 70 eV): m/z (%) = 714 (M^+, 100), 545 ($M^+ - C_3F_7$, 48), 376 ($M^+ - C_6F_{14}$, 49), 188 (65). mp 266 °C. HRMS (EI, 70 eV): found m/z (M^+), 714.0640, calculated for $C_{30}H_{12}F_{18}$, 714.0652.

Fabrication and Evaluation of OFETs. Top contact OFET devices with 50 μm channel lengths (L) and 1.5 mm channel widths (W) were fabricated on thermally oxidized, highly doped Si substrates. The gate insulator (SiO_2) was 210 nm thick. A thin film (50 nm thick) of FBP was vacuum deposited on the SiO_2 layer at a deposition rate of 0.1 nm s^{-1} under a pressure of 2×10^{-3} Pa at different substrate temperatures T_s = rt and 60 °C. Gold or silver source and drain electrodes were deposited on the semiconductor layer through a shadow mask. The FET characteristics were measured at rt under vacuum with an Agilent 6155C semiconductor parameter analyzer.

Results and Discussion

Synthesis and Molecular Characterization. In order to synthesize 2,9-disubstituted pentacene, it was necessary to utilize a scheme starting from pyromellic anhydride[21] rather than a conventional method involving the condensation of phthalaldehyde with 1,4-cyclohexanedione.[22] At first attempt, the synthetic route established for 2,9-dialkylpentacenes[21] was directly applied, where in the first step, Friedel–Crafts acylation of perfluorobutylbenzene with pyromellitic acid anhydride was involved. This direct acylation, however, afforded a complicated mixture of products due to the deactivated nature of perfluorobutylbenzene. Therefore, we adopted a modified route as shown in Figure 1, where the perfluorobutyl groups are introduced via Ulmann reaction of perfluorobutyl iodide with the bromo-substituted derivative after Friedel–Crafts acylation. In the first step (Friedel–Crafts acylation of bromobenzene), *ortho*-substituted by-products were also generated, but pure *para*-substituted product was easily obtained by recrystallization. Formation of the *ortho*-substituted derivative is mainly responsible for the low yield in this step. Esterification of the resulting terephthalic acid derivative was essential in order to avoid unexpected side reactions in the subsequent Ulmann reaction.

2,9-Bis(perfluorobutyl)pentacene (FBP) was obtained as a deep blue solid like the dialkyl analogues, and was slightly soluble in organic solvents such as toluene, tetrahydrofuran, and chloroform. Chemical structure was confirmed with MS, NMR, and IR spectroscopies. Improved solubility made it possible to measure ^{1}H and ^{19}F NMR spectra (in deuterated 1,1,2,2-tetrachloroethane at 100 °C). Signal patterns in the ^{1}H NMR spectrum are very similar to those of the dialkyl analogues, and all signals are shifted toward lower field (0.1–0.3 ppm), indicating that the strong σ electron-withdrawing perfluorobutyl substitution deacreases the electron density of the pentacene ring. In the IR spectrum, characteristic bands at 1219 and 1200 cm^{-1} associated with δ (C–F) in CF_3 and CF_2, respectively, which are absent in the IR spectrum of 2,9-dibutylpentacene (BP).[21]

Whereas this compound is relatively stable in the solid state, its solution was rather unstable and like dibutylpentacene bleached within 30 min when exposed to air and/or light. DSC analysis revealed that the melting point of FBP is 266 °C, which is higher than that of BP (115 °C)[21] suggesting that not only strong π–π interaction between pentacene rings but different chain–chain interactions between fluoroalkyl and alkyl substituents dominate cohesive forces in the solid state. Whereas the dialkyl analogue shows LC phase over a relatively wide temperature range (smectic; 115–194 °C), the fluorinated one shows no crystal–liquid crystal phase transition. This is probably due to the lack of flexibility in the perfluoroalkyl chains.

The introduction of fluoroalkyl groups enhanced the volatility. Figure 2 shows TGA thermograms measured at 1×10^{-4} Pa for FBP (a), BP (b), and unsubstituted pentacene (c). The onset points of weight loss for BP and pentacene were 282 and 286 °C, respectively. The effect of the alkyl chain is almost negligible. This result also suggests that volatility is predominantly determined by the π–π interaction between

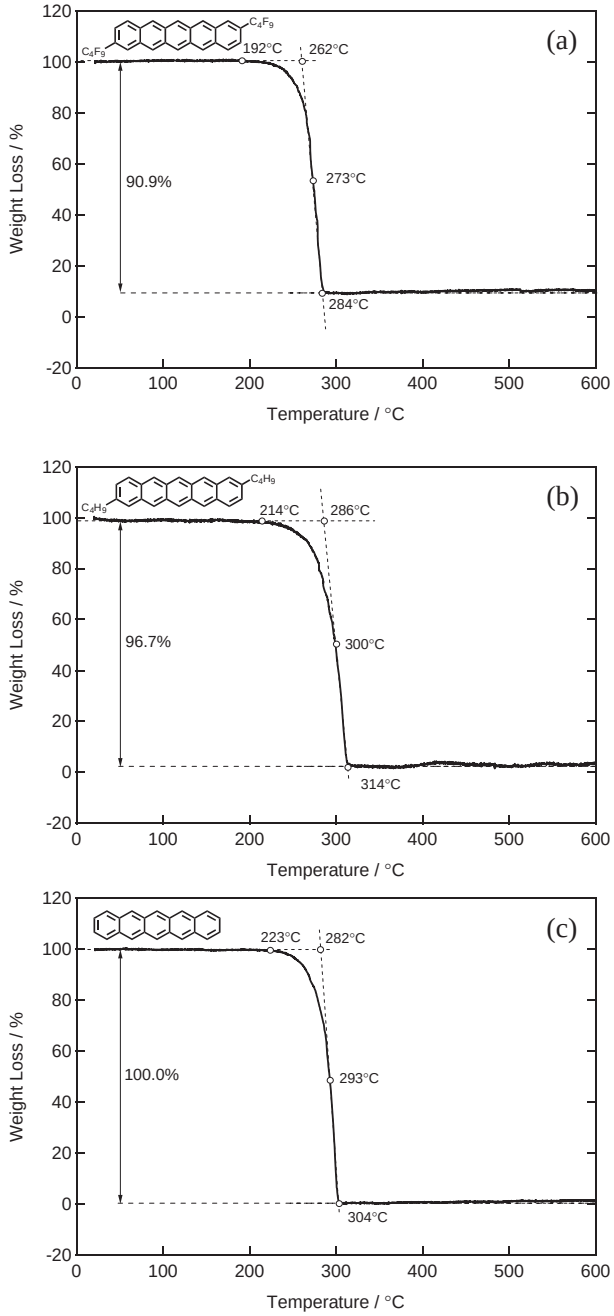

Figure 2. Thermogravimetric analysis graphs for (a) 2,9-bis(perfluorobutyl)pentacene, (b) 2,9-dibutylpentacene, and (c) pentacene. The heating rate is $10\,^{\circ}\mathrm{C\,min^{-1}}$ at 1×10^{-4} Pa.

pentacene rings. The onset point of weight loss for FBP was 262 °C under the same conditions. The enhancement of the volatility is also observed for fluorocarbon-substituted thiophene oligomers.[19a] In all cases, smooth TGA plots without inflection points were obtained, indicating that no decomposition occurred during evaporation. TGA under atomospheric pressure of nitrogen revealed that decomposition of 2,9-disubstituted pentacenes started beyond 350 °C.

Figure 3 shows UV–vis spectra for FBP and BP (a) in toluene solution and (b) on quartz substrate. In the UV–vis spectra in toluene solution, five characteristic absorption peaks appear periodically at 435, 470, 503, 539, and 584 nm for FBP, and this band splitting is probably due to vibronic coupling with one of the ν(C=C) stretching modes of the pentacene skeleton (1300–1400 $\mathrm{cm^{-1}}$).[24] Each peak shows slight bathochromic shifts compared with BP (429, 459, 496, 534, and 577 nm) in solution state. DFT calculations [RB3LYP/6-31G(d)] revealed that HOMO–LUMO gaps are 2.19 and 2.28 eV for fluoro and nonfluoro derivatives, respectively. Observed red shifts are consistent with the computed energy gap. The electron-accepting nature of the perfluoroalkyl chain affords a stronger effect on band gap modulation. In a film state, bathochromic shifts due to molecular aggregation were observed for both BP (646, 578, and 534 nm) and FBP (639, 572, and 531 nm) films compared with a solution state. Smaller red-shifts for FBP are probably due to loose interplaner stacking of pentacene rings because of the large van der Waals radius of fluorine.

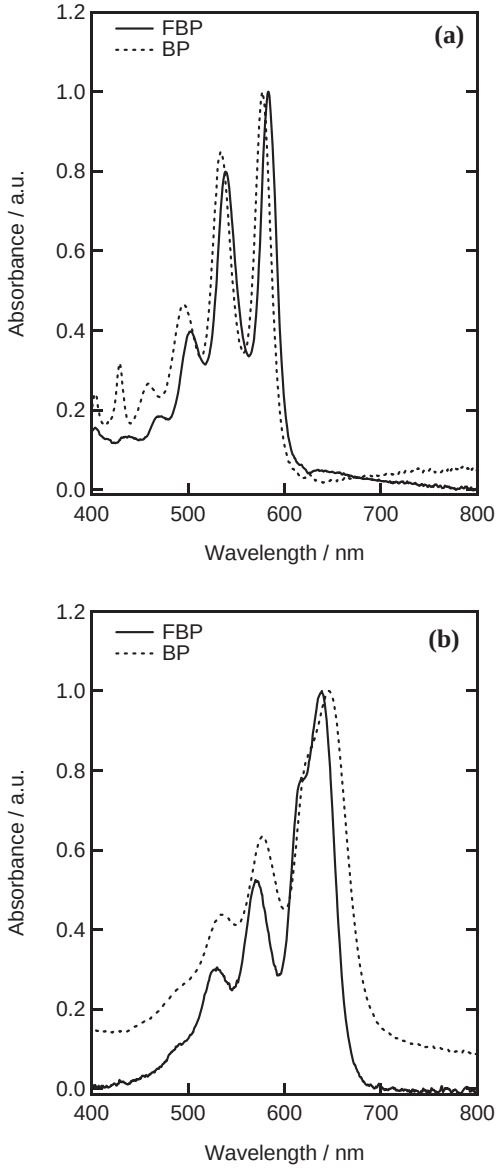

Figure 3. UV–vis spectra for 2,9-bis(perfluorobutyl)pentacene (FPB) and 2,9-dibutylpentacene (BP) (a) in toluene solution and (b) on quartz substrate.

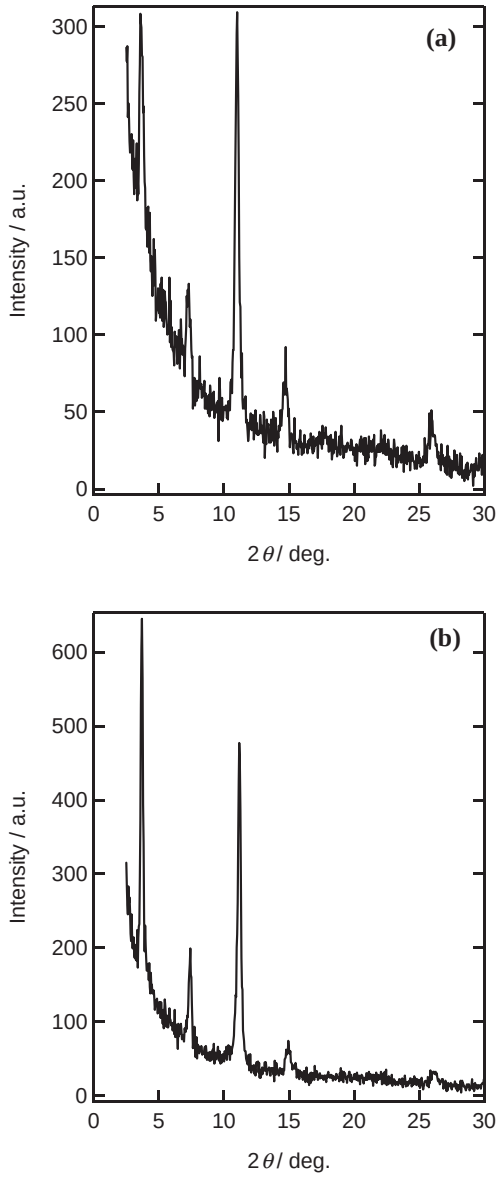

Figure 4. X-ray diffraction patterns from 2,9-bis(perfluorobutyl)pentacene thin films on SiO_2 substrate deposited at different substrate temperature of (a) room temperature and (b) 60 °C.

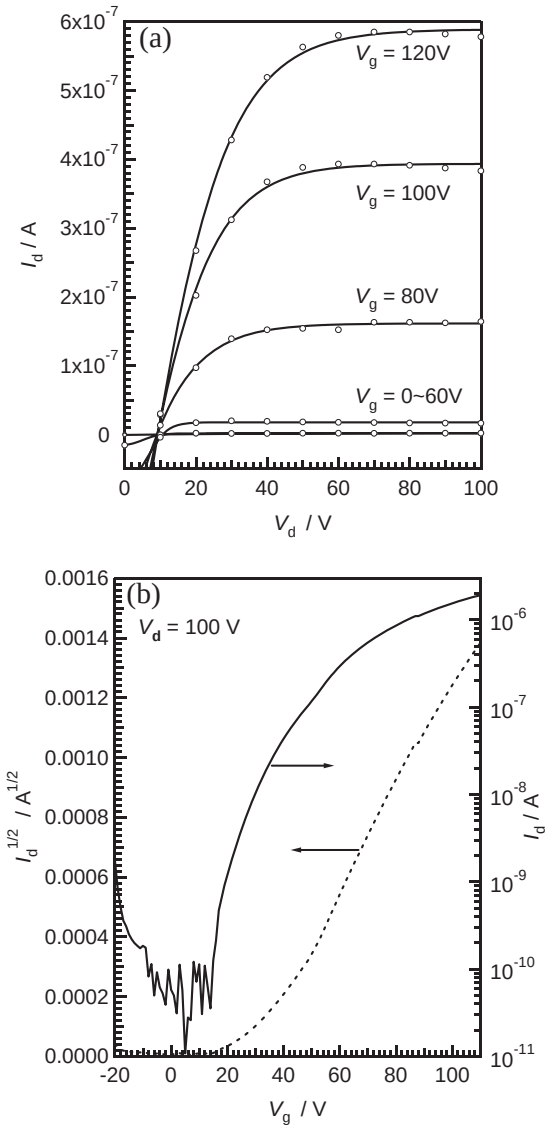

Figure 5. FET characteristics for 2,9-bis(perfluorobutyl)-pentacene based device fabricated at substrate temperature of 60 °C with Ag source and drain electrodes. (a) Drain current (I_d) vs. drain voltage (V_d) characteristics at various gate voltages (V_g), (b) $I_d{}^{1/2}$ and $\log I_d$ vs. V_g at $V_d = 100$ V.

Characteristics of Thin Films. AFM measurment of thin films of FBP deposited on SiO_2 at rt and 60 °C were performed. The size of crystal grains were not much different at different substrate temperatures. XRD measurements of the thin films afforded crucial information on the molecular orientation on the substrate. Figure 4 shows XRD patterns for FBP thin films deposited on SiO_2 at substrate temperature of (a) rt and (b) 60 °C. A primary diffraction peak at $2\theta = 3.6°$ and higher order peaks were observed in the patterns. At 60 °C, higher peak intensity was observed indicating that thin film with a high degree of ordering and crystallinity was obtained at higher temperature. The interlayer distance (d) estimated from the primary diffraction was 24.5 Å, which is nearly equal to computed molecular length (24 Å, corresponding to the long axis length of the projection in a plain parallel to a pentacene ring). This implies that pentacene cores are oriented with nearly upright structures on the substrate, which is suitable morphology for electrical transport between source and drain contacts in an FET.

Top contact configuration OFETs were fabricated with vapor-deposited FBP thin films, and mobility values were determined in the saturation regime by standard procedures.[25] Figure 5a shows drain current (I_d) vs. drain voltage (V_d) characteristics at various gate voltages (V_g) for an FBP-based OFET ($T_s = 60$ °C) with silver source and drain electrodes. The $I_d{}^{1/2}$ and $\log I_d$ vs. V_g characteristics of the device at $V_d = 100$ V are shown in Figure 5b. The OFET shows a typical output profile of a metal-oxide-semiconductor field-effect transistor. When the gate was biased positively, the drain current was observed as shown in Figure 5a. These results certainly indicate that accumulated electrons flow from the source to the drain through the channel region. Therefore, the OFET

Table 1. FET Characteristics of Devices Based on 2,9-Bis-(perfluorobutyl)pentacene

T_{sub}[a)]/°C	d–s Electrodes[b)]	Mobility/$cm^2\,V^{-1}\,s^{-1}$	I_{on}/I_{off}	V_{th}/V
rt	Au	2.1×10^{-6}	10	78
60	Au	4.1×10^{-6}	10	47
rt	Ag	2.6×10^{-5}	10	43
60	Ag	1.7×10^{-3}	10^4	33

a) Substrate temperature at vapor deposition. b) Drain and source electrode.

behaves in the n-channel accumulation mode. On the other hand, alkyl analogue (BP)-based OFETs showed no n-channel FET behavior. According to DFT MO calculations [RB3LYP/6-31G(d)], LUMO energy level for FBP (−2.96 eV) is more stabilized than that of BP (−2.27 eV), and this allows us to speculate that the energy barrier between the electrode and the semiconductor lowers by substitution with electron-withdrawing perfluorobutyl groups. The stabilization of HOMO energy level (FBP; −5.15 eV, BP; −4.49 eV) is responsible for no p-type FET response of FBP-based devices.

The mobility and the threshold voltage (V_{th}) were calculated from the slope and intercept, respectively, of the linear portion of the $I_d^{1/2}$ vs. V_g plot. Table 1 summarizes FET characteristics of FBP-based devices measured at room temperature under vacuum (no FET response was observed in air). When the substrate temperature increased to 60 °C, V_{th} was extensively reduced for gold and silver electrodes due to the better contact between electrodes and semiconductor. As mentioned above (Figure 4), the better ordered film with larger grain size was obtained at 60 °C. When source and drain electrodes were changed from gold to silver, the electron mobility was improved from 2.1×10^{-6} to 2.6×10^{-5}, and 4.1×10^{-6} to $1.7 \times 10^{-3}\,cm^2\,V^{-1}\,s^{-1}$ at room temperature and 60 °C, respectively, in FBP deposition, and a slight decrease of the V_{th} values was also observed. A larger I_{on}/I_{off} ratio was observed for a device with silver electrodes fabricated at 60 °C. It is considered that silver electrodes with a lower work function (4.26 eV) than that of gold (5.10 eV) lowered the injection barrier between the electrode and semiconducting layer, and the field-effect mobility concomitantly increased as reported for OFET devices based on partially fluorinated dibenzodithiophene derivatives.[26] It was found that the substitution of p-type pentacene core with perfluoroalkyl groups affords n-type material.

Conclusion

We successfully synthesized novel 2,9-bis(perfluorobutyl)-pentacene utilizing a modified synthetic scheme established for the synthesis of 2,9-dialkylpentacenes. It was found that the substitution of the pentacene core with perfluorobutyl groups enhances volatility and electron affinity compared with 2,9-dibutylpentacene. We have firstly demonstrated that the introduction of perfluoroalkyl groups is an effective way to convert a p-type parent core to n-type material in the pentacene family. Observed mobility values are still lower than that of high-performance n-type organic materials like perfluoropentacene and thiazole oligomers, but the efforts including the optimization of the length of perfluoroalkyl group, and the surface modification of the dielectric layer are now in progress in order to improve the performance.

References

1 J. A. Rogers, Z. Bao, *J. Polym. Sci., Part A: Polym. Chem.* **2002**, *40*, 3327.

2 P. F. Baude, D. A. Ender, M. A. Haase, T. W. Kelley, D. V. Muyres, S. D. Theiss, *Appl. Phys. Lett.* **2003**, *82*, 3964.

3 M. Kitamura, T. Imada, Y. Arakawa, *Appl. Phys. Lett.* **2003**, *83*, 3410.

4 J. E. Anthony, *Chem. Rev.* **2006**, *106*, 5028.

5 H. Meng, M. Bendikov, G. Mitchell, R. Helgeson, F. Wudl, Z. Bao, T. Siegrist, C. Kloc, C. H. Chen, *Adv. Mater.* **2003**, *15*, 1090.

6 T. Takahashi, M. Kitamura, B. Shen, K. Nakajima, *J. Am. Chem. Soc.* **2000**, *122*, 12876.

7 J. Reichwagen, H. Hopf, J.-P. Desverge, A. D. Guerzo, H. Bouas-Laurent, *Synthesis* **2005**, 3505.

8 H. Tian, J. Shi, B. He, N. Hu, S. Dong, D. Yan, J. Zhang, Y. Geng, F. Wang, *Adv. Funct. Mater.* **2007**, *17*, 1940.

9 Z. Bao, A. Dobabalapur, A. J. Lovinger, *Appl. Phys. Lett.* **1996**, *69*, 4108.

10 B. Crone, A. Dodabalapur, Y. Y. Lin, R. W. Filas, Z. Bao, R. Sarpeshkar, H. E. Katz, W. Li, *Nature* **2000**, *403*, 521.

11 C. Rost, D. J. Gundlach, S. Karg, W. Riess, *J. Appl. Phys.* **2004**, *95*, 5782.

12 T.-W. Lee, Y. Byun, B.-W. Koo, I.-N. Kang, Y.-Y. Lyu, C. H. Lee, L. Pu, S. Y. Lee, *Adv. Mater.* **2005**, *17*, 2180.

13 Z. Bao, A. J. Lovinger, J. Brown, *J. Am. Chem. Soc.* **1998**, *120*, 207.

14 T. M. Pappenfus, R. J. Chesterfield, C. D. Frisbie, K. R. Mann, J. Casado, J. D. Raff, L. L. Miller, *J. Am. Chem. Soc.* **2002**, *124*, 4184.

15 H. E. Katz, A. J. Lovinger, J. Johnson, C. Kloc, T. Siegrist, W. Li, Y. Y. Lin, A. Dodabalapur, *Nature* **2000**, *404*, 478.

16 P. R. L. Malenfant, C. D. Dimitrakopoulos, J. D. Gelorme, L. L. Kosbar, T. O. Graham, A. Curioni, W. Andreoni, *Appl. Phys. Lett.* **2002**, *80*, 2517.

17 S. Ando, R. Murakami, J. Nishida, H. Tada, Y. Inoue, S. Tokito, Y. Yamashita, *J. Am. Chem. Soc.* **2005**, *127*, 14996.

18 Y. Sakamoto, T. Suzuki, M. Kobayashi, Y. Gao, Y. Fukai, Y. Inoue, F. Sato, S. Tokito, *J. Am. Chem. Soc.* **2004**, *126*, 8138.

19 a) A. Facchetti, M. Mushrush, H. E. Katz, T. J. Marks, *Adv. Mater.* **2003**, *15*, 33. b) A. Facchetti, M.-H. Yoon, C. L. Stern, G. R. Hutchison, M. A. Ratner, T. J. Marks, *J. Am. Chem. Soc.* **2004**, *126*, 13480. c) A. Facchetti, M. Mushrush, M.-H. Yoon, G. R. Hutchison, M. A. Ratner, T. J. Marks, *J. Am. Chem. Soc.* **2004**, *126*, 13859.

20 J. A. Letizia, A. Facchetti, C. L. Stern, M. A. Ratner, T. J. Marks, *J. Am. Chem. Soc.* **2005**, *127*, 13476.

21 K. Okamoto, T. Kawamura, M. Sone, K. Ogino, *Liq. Cryst.* **2007**, *34*, 1001.

22 a) V. Bruckner, J. Tomasz, *Acta Chim. Hung.* **1961**, *28*, 405. b) H. Meng, M. Bendikov, G. Mitchell, R. Helgeson, F. Wudl, Z. Bao, T. Siegrist, C. Kloc, C.-H. Chen, *Adv. Mater.* **2003**, *15*, 1090.

23 B. Wex, B. R. Kaafarani, R. Schroeder, L. A. Majewski, P. Burckel, M. Grell, D. C. Neckers, *J. Mater. Chem.* **2006**, *16*, 1121.

24 T. Minakata, Y. Natsume, *Synth. Met.* **2005**, *153*, 1.

25 C. D. Dimitrakopoulos, P. R. L. Malenfant, *Adv. Mater.* **2002**, *14*, 99.

26 K. Takimiya, Y. Kunugi, H. Ebata, T. Otsubo, *Chem. Lett.* **2006**, *35*, 1200.